Original Report: Laboratory Investigation

American Journal of Nephrology

Am J Nephrol 2010;32:340–346
DOI: 10.1159/000319444

Received: May 13, 2010
Accepted: July 15, 2010
Published online: August 20, 2010

Characterization of Stx2 Tubular Response in a Rat Experimental Model of Hemolytic Uremic Syndrome

F. Ochoa[a] N.R. Lago[b] E. Gerhardt[a] C. Ibarra[a] E. Zotta[a]

[a]Laboratorio de Fisiopatogenia, Departamento de Fisiología, y [b]Centro de Patología, Departamento de Patología, Facultad de Medicina, Universidad de Buenos Aires, Buenos Aires, Argentina

Key Words

Hemolytic uremic syndrome · Shiga toxin · Acute renal failure · Transforming growth factor-beta1 · Alpha-smooth muscle actin · Epithelial markers

Abstract

Background/Aims: In Argentina, hemolytic uremic syndrome (HUS) constitutes the most frequent cause of acute renal failure in children. The aim of our study was to analyze the early tubular response under the effect of Shiga toxin type 2 (Stx2) in a rat experimental model of HUS. ***Methods:*** Adult male Sprague-Dawley rats were injected intraperitoneally with culture supernatant from recombinant *Escherichia coli* expressing Stx2. Functional, histological, immunohistochemical and Western blot studies were performed at 48 h postinoculation. ***Results:*** Renal tubules showed the loss of the epithelial markers E-cadherin and β-catenin, and an increase in transforming growth factor-β1 expression. We detected the expression of α-smooth muscle actin in the interstitium and fibrosis in the periglomerular areas. ***Conclusion:*** Our results indicate that the early tubular response to the effects of Stx2 is related to an immunophenotype change of tubular cells and the presence of mild fibrosis in the interstitium.

Introduction

Hemolytic uremic syndrome (HUS) is a disease defined by thrombotic microangiopathy, hemolytic anemia, thrombocytopenia, and acute renal failure (ARF). HUS associated with diarrhea is caused by Shiga toxin (Stx)-producing *Escherichia coli*. HUS constitutes the most common cause of ARF in Argentina. Approximately 2–4% of patients die during the acute phase, and one third out of the 96% who survive are at risk of having chronic renal sequelae [1]. However, the pathophysiology of ARF during HUS is not well understood.

During ARF, proinflammatory cytokines such as tumor necrosis factor-α (TNF-α) and transforming growth factor-β1 (TGF-β1) may contribute to evolving renal disease [2]. TGF-β is involved in many of the events that are observed during renal repair and is also related to the development of fibrosis in several pathologies [3, 4]. Hyperactive TGF-β1 signaling under pathological conditions is related to the development of immunophenotype cell changes that acquire new characteristic features of the mesenchyme [3, 4]. The loss of epithelial markers such as the cadherin/catenin complex, an essential regulator of both intercellular adhesion and epithelial cell polarity, and the increase in the mesenchymal markers in tubular cells from several kidney diseases have been reported [5–

KARGER

Fax +41 61 306 12 34
E-Mail karger@karger.ch
www.karger.com

0250–8095/10/0324–0340$26.00/0

Accessible online at:
www.karger.com/ajn

Elsa Zotta
Departamento de Fisiología, Facultad de Medicina
Paraguay 2155, 7mo piso
Buenos Aires 1121 (Argentina)
Tel. +54 11 5950 9500, int. 2141, E-Mail ezotta@fmed.uba.ar

7]. Furthermore, the increase in the expression of α-smooth muscle actin (α-SMA), a marker of myofibroblasts, predicts progressive renal dysfunction in human and experimental models of renal disease [8]. That tubular phenomena are occurring in the early phase of HUS has not yet been described. In an experimental model of HUS in rats, we hypothesize that inflammatory factors released during the first 48 h of acute kidney injury induced by Stx2 could be related to the interstitial changes.

Materials and Methods

Adult male Sprague-Dawley rats (150 ± 3 g body weight) were obtained from the animal facility of the School of Pharmacy and Biochemistry, University of Buenos Aires, Argentina. The rats were housed individually under controlled conditions of light/dark, humidity, and temperature, with food and water available ad libitum.

Experimental Protocols

Rats were randomly divided into two groups of 8 rats. Experimental HUS was induced as previously described [9]. Briefly, rats from the experimental group (Stx2-treated rats) were injected intraperitoneally with recombinant *Escherichia coli* culture supernatant (sStx2) containing Stx2 (20 μg/kg body weight). Control rats were inoculated with the same volume of culture supernatant that did not contain Stx2.

sStx2 was obtained as previously described having a cytotoxicity of 2×10^4 CD_{50}/ml (1 CD_{50} = 40 pg/ml) [10]. The LPS content in the supernatant determined by the HEK-Blue LPS Detection Kit (Invitrogen, San Diego, Calif., USA) was 70 ng LPS/μg Stx2 protein.

All rats were kept in cages for 48 h with free access to water and food and with control of the light/dark cycle and temperature.

Renal Functions

To recollect the urine volume rats were kept in metabolic cages for 48 h with free access to water and food and under a controlled light/dark cycle and temperature. Blood samples were obtained from rats by cardiac puncture prior to sacrifice. Creatinine and urea plasma concentrations were assessed using a commercial kit (Wiener Lab, Argentina).

Light Microscopy

Rats were anesthetized (100 μg ketamine and 10 μg diazepam/g body weight, intraperitoneally) and perfused with 4% paraformaldehyde in phosphate-buffered saline (PBS). Kidneys were removed and tissues were fixed in formol buffer 10% in PBS 0.1 M (pH 7.4). The tissue sections were dehydrated and included in paraffin. Sagittal cuts (5 μm) were made with a microtome (Leica RM 2125, Wetzlar, Germany) and mounted on 2% silane-coated slides. The slides were stained with Mallory's trichrome and observed by light microscopy (Nikon Eclipse 200, N.Y., USA).

Immunoperoxidase

Samples were blocked of endogenous peroxidase with H_2O_2 0.3% for 10 min. Later, the slides were preincubated with no immune rabbit serum, diluted in PBS (1:100) at room temperature for 30 min and incubated with the primary antibodies: anti-TGF-β1 (1:100, Santa Cruz Biotechnology), anti-E-cadherin (1:100, Dako, USA), anti β-catenin (1:100, Dako), in a humidity chamber at 4°C overnight. The immunoperoxidase technique was then performed following the protocol from the RTU Vectastain Kit (Vector, Peterborough, UK). The antigen was revealed by diaminobenzidine (DAB, Vector). Finally, the sections were counterstained and mounted for observation.

Immunofluorescence

The slides were preincubated with no immune rabbit serum in PBS (1:100) at room temperature for 30 min, following by incubation with a monoclonal anti-smooth muscle α-actin (α-SMA 1:100, Dako, USA) antibody overnight in a wet chamber at 4°C. After several rinses in PBS, the slides were incubated with an antimouse biotinylated IgG antibody (1:200; GE Healthcare, USA) for 1 h and then incubated with streptavidin-Texas red and conjugated (1:100, GE Healthcare, USA) for 1 h at room temperature in a wet chamber. Finally, all the slides were mounted on a mixture containing PBS:glycerol (1:3), and observed in an epifluorescent microscope (Nikon Eclipse E200). Negative controls were performed without primary antibodies.

Western Blot

The renal cortex was micro-dissected and homogenized in buffer (10 mM triethanolamine, 250 mM sucrose, pH 7.6) with proteinase inhibitors. The protein concentration was determined with the BCA Protein Assay Kit (Pierce Biotechnology Inc., Rockford, Ill., USA). Samples of 100 μg were electrophoresed using 12.5% gels and electroblotted. Blots were incubated with rabbit polyclonal anti-TGF-β1 antibody (1:1,000) and horseradish peroxidase-conjugated goat antirabbit IgG antibody (1:3,000 Bio-Rad, Hercules, Calif., USA). Then membranes were incubated with mouse monoclonal antihuman α-SMA antibody (1:1,000) and with horseradish peroxidase-conjugated rabbit antimouse IgG antibody (1:3,000 Sigma-Aldrich Co., Saint Louis, Mo., USA). To determine the uniformity of loading, protein blots were probed with the monoclonal anti-β-actin antibody (1:1,000 Sigma-Aldrich). Band intensities were measured using the Quantity One densitometry software package (BioRad). Protein bands were normalized to their respective β-actin bands. The immunoblot analysis was carried out on three different tissue preparations from three independent experiments.

Measurement of Fibrosis and E-Cadherin and β-Catenin Expression

Ten separate fields of each section stained by Mallory-trichrome and immunohistochemistry using E-cadherin and β-catenin antibodies were scanned at ×200 magnifications, put into digital form and analyzed using imaging software (Image Pro Plus, Media Cybernetics, USA) [11]. Mallory's trichrome technique detects areas of fibrosis stained in blue.

Statistical Analysis

Data shown are mean ± SEM. The statistical significance between two mean values obtained for two different experimental conditions was calculated by Student's t test. $p < 0.05$ was considered significant.

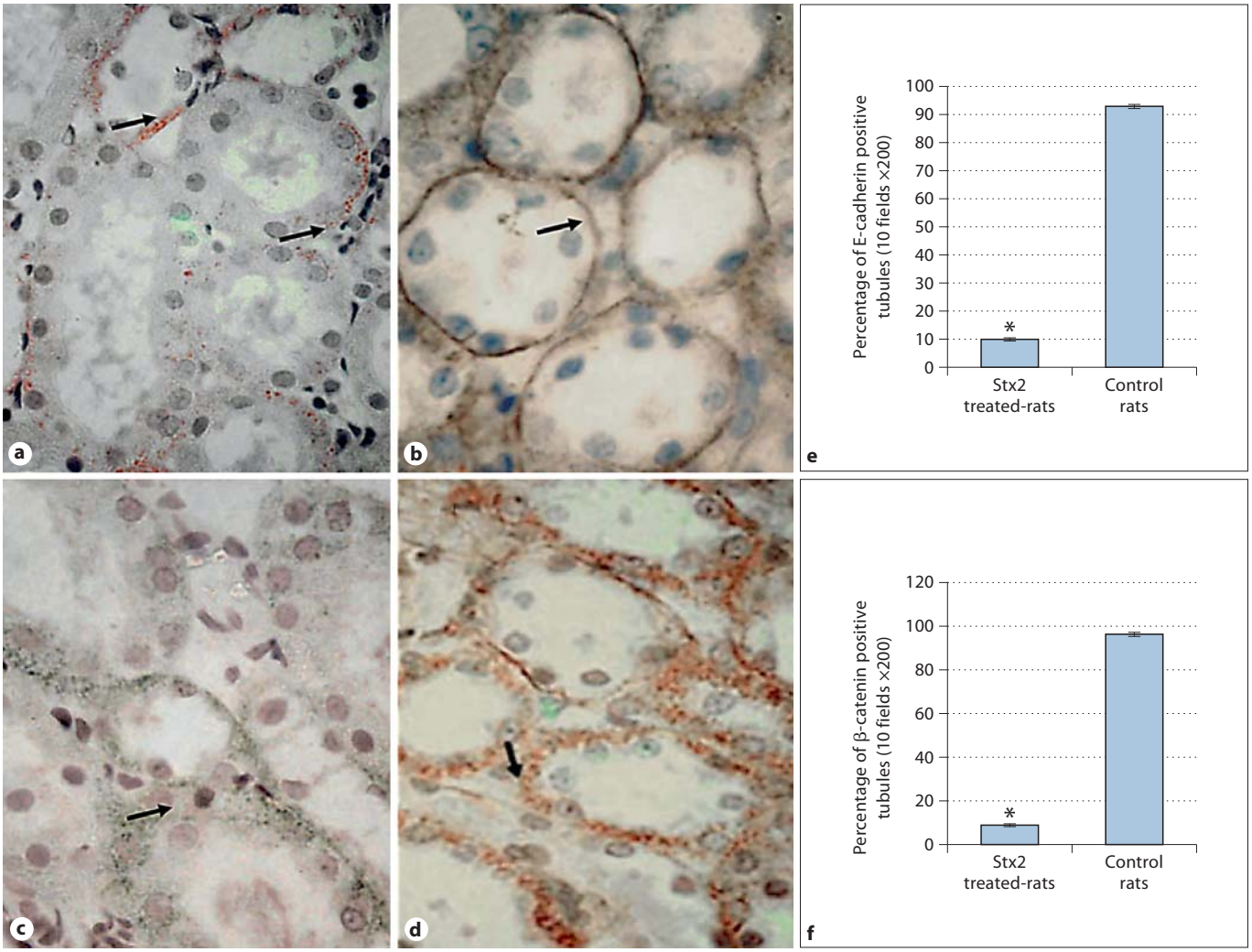

Fig. 1. Expression of the epithelial markers E-cadherin and β-catenin by immunohistochemistry. The expression of E-cadherin is significantly decreased in renal tubules from experimental rats undergoing the effect of Stx2 (**a**, black arrows) as compared to control rats (**b**). β-Catenin is found in cytoplasmic granules localized in perinuclear areas (**c**, black arrow) in experimental rats as compared to controls (**d**). ×1,000. Using a grid superimposed on the image, the number of tubules positive for E-cadherin and β-catenin was counted, and the percentage was measured. Expression of E-cadherin (10.1 ± 0.7 vs. 93.2 ± 0.5%; $p < 0.001$, n = 10, **e**) and β-catenin (9.2 ± 0.5 vs. 96.5 ± 0.8%; $p < 0.001$, n = 10, **f**) were significantly decreased with respect to the controls.

Results

A significant increase in creatinine (115 ± 3 vs. 38 ± 2 μmol/l, $p < 0.01$ n = 8) and urea (27 ± 2 vs. 5 ± 1 mmol/l, $p < 0.01$, n = 8) plasma concentrations was observed 48 h after sStx2 treatment. Urine volume was increased in the first 24 h after treatment (32.1 ± 1.3 vs. 20.4 ± 3.2 ml/day, $p < 0.05$, n = 8) but in the next 24 h (48 h after treatment) returned to normal levels (14.8 ± 3.1 vs. 18. 7 ± 2.0 ml/day, n = 8).

Immunohistochemistry of tubular epithelial cells from sStx2-treated rats at 48 h showed a decrease in the expression of E-cadherin and β-catenin in the membrane and cytoplasm (fig. 1a, c). Perinuclear localization of β-catenin was observed in several tubule cells. In cortex, morphometric quantification detected a significantly decrease in the expression of E-cadherin (10.1 ± 0.7 vs. 93.2 ± 0.5%; $p < 0.001$, n = 10) and β-catenin (9.2 ± 0.5 vs. 96.5 ± 0.8%; $p < 0.001$, n = 10) in respect to the controls (fig. 1e, f).

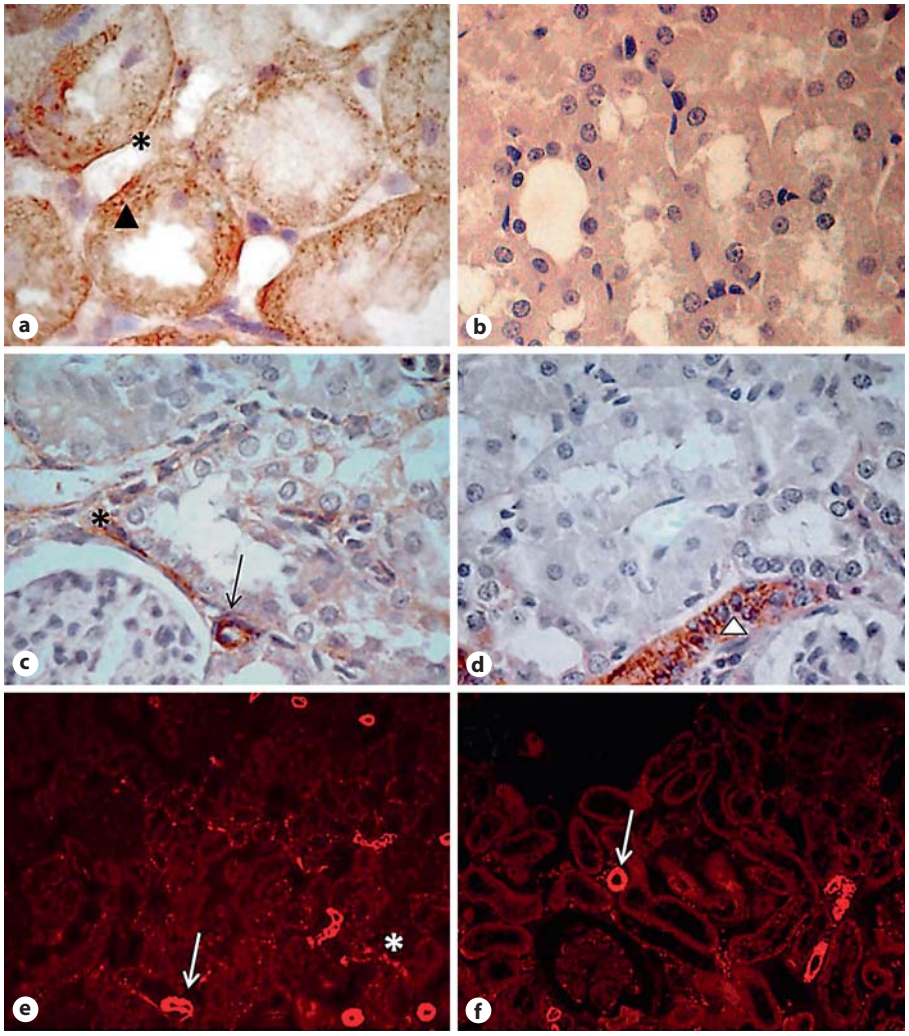

Color version available online

Fig. 2. Tubular response to the injury. TGF-β1 is expressed in the basolateral membranes (asterisk in **a**) and the cytoplasm (arrowhead in **a**) of epithelial tubular cells from the experimental rats. TGF-β1 was negative in the control group (**b**). α-SMA was expressed in smooth muscle vessels from control rats (white arrowhead in **d**, white arrow in **f**). De novo labeling was observed in vessels and interstitium (black arrow in **c**, white arrow in **e**) and interstitium (black asterisk in **c**, white asterisk in **e**) of experimental rats. **a**, **b** Immunoperoxidase, ×1,000. **c**, **d** Immunoperoxidase, ×400. **e**, **f** Immunofluorescence, ×200.

Injured renal tubules showed strong labeling of TGF-β1 in the basolateral membranes and cytoplasm (fig. 2a) as well as labeling of α-SMA in the interstitial fibroblasts and vessels (fig. 2c, e). In control rats, TGF- β1 was not detected and α-SMA was observed only in the vessels (fig. 2d, f).

In order to determine whether the presence of α-SMA is related to the development of interstitial fibrosis, Mallory's trichrome staining was performed. Areas of fibrosis were detected around the glomeruli and renal tubules (fig. 3a, b). Morphometric quantification showed a significant increase in areas of periglomerular fibrosis in Stx2-treated rats with respect to the controls (8.0 ± 0.6 vs. 0.9 ± 0.3%, n = 14) (fig. 3c).

Western blot analysis performed in renal cortex from Stx2-treated rats using anti-TGF-β1 antibody showed 3 protein bands at approximately 12.5, 52 and 105 kDa with a different expression pattern when compared with that observed in control rats (fig. 4a). The 12.5-kDa band corresponding to the monomeric active form of TGF-β1 was more abundant, whereas the 52- and 105-kDa bands were less abundant in the Stx2-treated rats than in the control group (fig. 4b). A different α-SMA expression was also observed. An increase in the 42-kDa band in renal cortex from the Stx2-treated compared with the control rats was observed in renal tubules and the interstitium (fig. 4c, d).

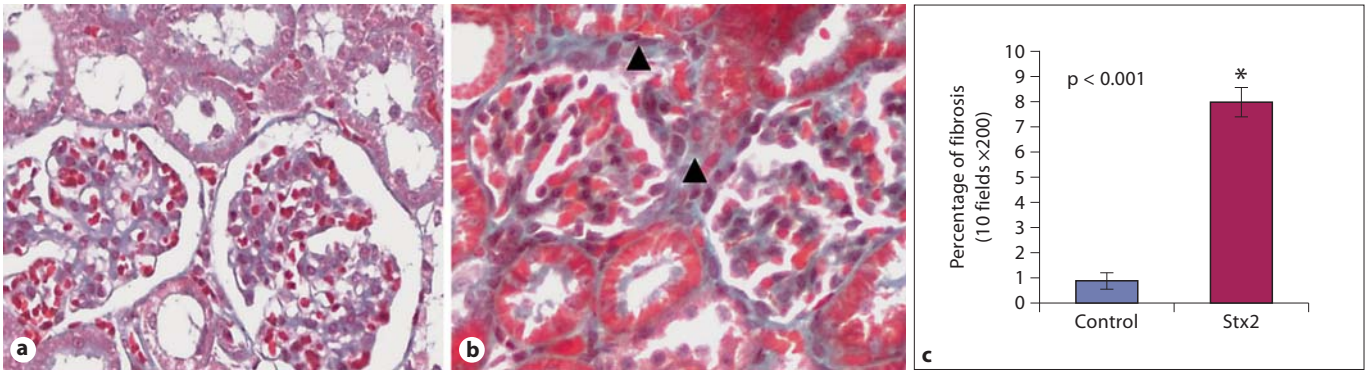

Fig. 3. Fibrosis detection. Areas of periglomerular fibrosis stained in blue were observed in Stx2-treated rats (**b**, black arrowheads) as compared to controls (**a**). Mallory's trichrome. ×200. Using a grid superimposed on the image, the number of points overlapping the blue collagen staining was counted, and the percentage of blue collagen area in the examined tubulointerstitium was measured. Periglomerular fibrosis was significantly increased with respect to the controls (8.0 ± 0.6 vs. 0.9 ± 0.3%; $p < 0.001$, $n = 14$, **c**).

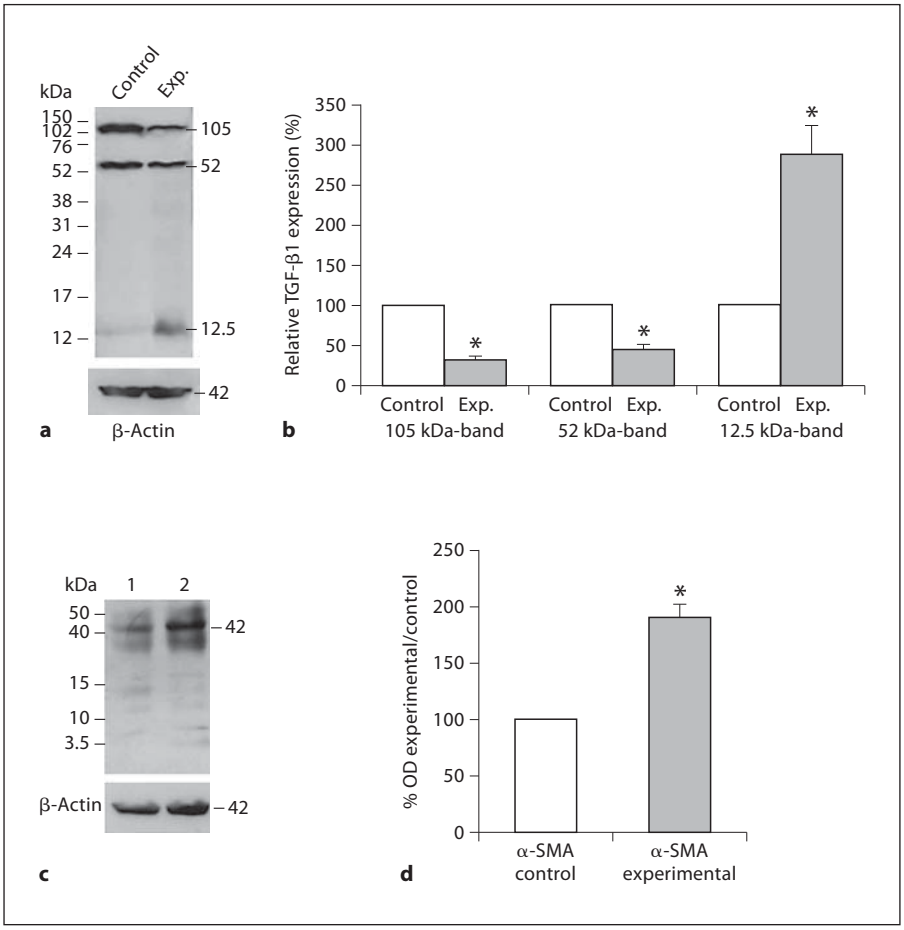

Fig. 4. TGF-β1 immunodetection by Western blot. **a** Representative blots of TGF-β1 expression in renal cortex. **b** Bar graphs representing average protein levels normalized to the internal control β-actin. Note that a 12.5-kDa band corresponding to the active form of TGF-β1 increased and that upper bands at 52 and 105 kDa corresponding to the precursor form of TGF-β1 decreased in the experimental rats as compared to controls. **c** Expected 42-kDa band corresponding to α-SMA. The intensities of the bands were quantified by Image J software (**d**). Note that the 42-kDa band increased in the cortex of experimental rats (lane 2) when compared to controls (lane 1). These results are representative of 4 rats from each group (* $p <$ 0.05).

Discussion

In the present study, we have studied the early epithelial renal tubular response during acute renal injury in an experimental model of HUS in rats.

In agreement with our previous findings, Stx2-treated rats developed an increase in creatinine and urea plasma concentrations were used as markers of renal dysfunction. Urine volume showed similar modifications as reported previously indicating not only tubular but also glomerular dysfunction [9].

Western blot analyses showed that TGF-β1 protein was differentially expressed in Stx2-treated rats with respect to the controls. The temporal expression of TGF-β1 and its effects during the early stage of HUS nephropathy have not yet been clearly defined although it is known that hyperactive TGF-β1 signaling under pathological conditions is related to the development of cellular changes such as loss of their epithelial phenotype [5, 8]. The activation of TGF-β1 in vivo has also been described in the evolution of the chronic renal sequelae [12–14]. According to this finding, the 12.5-kDa band corresponding to the active form of TGF-β1 increased [15, 16] whereas the 52- and 105 kDa-bands corresponding to the precursor's forms of TGF-β1 decreased in the Stx2-treated rats compared with the controls. A similar early response has been described in cultured tubular epithelial cells after 6 h of TGF-β1 incubation [15–17]. Alterations in the physiology due to the effect of autocrine/paracrine TGF-β activity were localized predominantly in the proximal tubule of the injured and regenerating kidney in a model of ischemia-reperfusion in rats [18]. In another model of ARF, Lebeau et al. [19] demonstrated that the proximal tubular dysfunction could be detected as early as 2 days after aristolochic acid administration, and a more pronounced intoxication may lead to severe tubular atrophy and interstitial fibrosis with an increase of TGF-β1 expression in the tubulointerstitial areas. Taken together with these data, our results suggest that the tubular epithelial cells affected by Stx2 may be the targets of the focal activation of TGF-β1 at 48 h. Moreover, a decrease in the expression of E-cadherin and β-catenin at 48 h indicates an immunophenotype change in tubular cells that could be induced by TGFβ1. Recent studies have provided evidence that the immunophenotype change could contribute to the generation of kidney fibroblasts during experimental renal fibrosis [20].

In our model, we detected a development of mild fibrosis and a significant increase of α-SMA after 48 h of sStx2 treatment. The origin of these cells may be in the activation of interstitial resident fibroblasts, hemopoietic or mesenchymal stem cells migrant from flat bones, and epithelial to mesenchymal transition [21]. Recent reports have described similar results in other animal models. A mouse ureteral obstruction model progressed to a tubule-interstitial fibrosis after 24 h treatment showing TGF-β1 signaling in renal tubules [22]. Injection of cyclosporine induced the development of fibrosis and the expression of TGF-β1 [23]. Indeed, an early tendency towards fibrosis (fast fibrosis) similar to the one described here has been detected in renal biopsies with acute tubular necrosis [24]. Although it has been described that the immunophenotype changes are suggestive of an epithelial-to-mesenchymal transition [25] other mechanisms of renal fibrosis cannot be discarded such as the production of tubular chemokines with stimulation of interstitial fibroblasts [26].

Despite the mechanism of the development of incipient fibrogenesis requiring further studies, our results suggest that the immunophenotype changes could be associated to an activated state of tubular cells. So, the development of fast fibrosis in the renal interstitium could be related to the response to the injury produced by sStx2.

In summary, we report for the first time in a rat experimental model of HUS an induction of immunophenotype changes in renal tubules, a modification in the TGF-β protein expression pattern, an increase in the expression of α-SMA in interstitium and a development of incipient fibrosis during the first 48 h of chronic renal disease. Further studies will be necessary to determine whether this response could be responsible for the evolution to the chronic renal disease characteristic of HUS.

Acknowledgements

The University of Buenos Aires (M030, M827), the National Council of Research (CONICET, PIP 5587) and the ANPCYT (PICT-26224) supported this work. We gratefully acknowledge the excellent assistance of Claudio Mirabelli from GEMA-BIOTECH S.A.

References

1 Repetto HA: Epidemic hemolytic-uremic syndrome in children. Kidney Int 1997;52:1708–1719.

2 Zager RA, Johnson AC, Lund S: Uremia impacts renal inflammatory cytokine gene expression in the setting of experimental acute kidney injury. Am J Physiol Renal Physiol 2009;297:F961–F970.

3 Ziyadeh FN: Different roles for TGF-β and VEGF in the pathogenesis of the cardinal features of diabetic nephropathy. Diabetes Res Clin Pract 2008;82:S38–S41.

4 Basile DP: The TGF-β system in kidney disease and repair: recent progress and future directions. Curr Opin Nephrol Hypertens 1999;8:21–30.

5 Jiang J, Dean D, Burghardt RC, Parrish AR: Disruption of cadherin/catenin expression, localization, and interactions during $HgCl_2$-induced nephrotoxicity. Toxicol Sci 2004;80:170–182.

6 Tyler JR, Robertson H, Booth TA, Burt AD, Kirby JA: Chronic allograft nephropathy: Intraepithelial signals generated by transforming growth factor-beta and bone morphogenetic protein-7. Am J Transplant 2006;6:1367–1376.

7 Rastaldi MP, Ferrario F, Giardino L, Dell'Antonio G, Grillo C, Grillo P, Strutz F, Muller GA, Colasanti G, D'Amico G: Epithelial-mesenchymal transition of tubular epithelial cells in human renal biopsies. Kidney Int 2002;62:137–146.

8 Neilson EG: Mechanisms of disease: fibroblasts – a new look at an old problem. Nat Clin Pract Nephrol 2006;2:101–108.

9 Zotta E, Lago N, Ochoa F, Repetto HA, Ibarra C: Development of an experimental hemolytic uremic syndrome in rats. Pediatr Nephrol 2008;23:559–567.

10 Pistone Creydt V, Fernandez Miyakawa M, Martín F, Zotta E, Silberstein C, Ibarra C: Shiga toxin 2B subunit inhibits net fluid absorption in human colon and elicits fluid accumulation in rat colon loops. Braz J Med Biol Res 2004;37:799–808.

11 Mizuguchi Y, Miyajima A, Kosaka T, Asano T, Asano T, Hayakawa M: Atorvastatin ameliorates renal tissue damage in unilateral ureteral obstruction. J Urol 2004;172:2456–2459.

12 Sutaria PM, Ohebshalom M, McCaffrey TA, Vaughan ED Jr, Felsen D: Transforming growth factor-beta receptor types I and II are expressed in renal tubules and are increased after chronic unilateral ureteral obstruction. Life Sci 1998;62:1965–1972.

13 Crawford SE, Stellmach V, Murphy-Ullrich JE, Ribeiro SM, Lawler J, Hynes RO, Boivin GP, Bouck N: Thrombospondin-1 is a major activator of TGF-beta1 in vivo. Cell 1998;93:1159–1170.

14 Molitoris BA, Marrs J: The role of cell adhesion molecules in ischemic acute renal failure. Am J Med 1999;106:583–592.

15 Massagué J, Cheifetz S, Laiho M, Ralph DA, Weis FM, Zentella A: Transforming growth factor-β. Cancer Surv 1992;12:81–103.

16 Hyytiainen M, Penttineen C, Keski-Oja J: Latent TGF-β binding proteins: extracellular matrix association and roles in TGF-β activation. Crit Rev Clin Lab Sci 2004;4:233–264.

17 Kalluri R, Zeisberg M: Exploring the connection between chronic renal fibrosis and bone morphogenic protein-7. Histol Histopathol 2003;18:217–224.

18 Spurgeon KR, Donohoe DL, Basile DP: Transforming growth factor-β in acute renal failure: receptor expression, effects on proliferation, cellularity, and vascularization after recovery from injury. Am J Physiol Renal Physiol 2005;288:F568–F577.

19 Lebeau C, Debelle FD, Arlt VM: Early proximal tubule injury in experimental aristolochic acid nephropathy: functional and histological studies. Nephrol Dial Transplant 2005;20:2321–2332.

20 Iwano M, Plieth D, Danoff TM, Xue C, Okada H, Neilson EG: Evidence that fibroblasts derive from epithelium during tissue fibrosis. J Clin Invest 2002;110:341–350.

21 Yang J, Liu Y: Dissection of key events in tubular epithelial to myofibroblast transition and its implications in renal interstitial fibrosis. Am J Pathol 2001;159:1465–1475.

22 Yang JW, Shultz RW, Mars WM, Wegner RE, Li Y, Dai C, Nejak K, Liu Y: Disruption of tissue-type plasminogen activator gene in mice reduces renal interstitial fibrosis in obstructive nephropathy. J Clin Invest 2002;110:1525–1538.

23 Slattery C, Campbell E, McMorrow T, Ryan MP: Cyclosporine A-induced renal fibrosis: a role for epithelial-mesenchymal transition. Am J Pathol 2005;167:395–407.

24 Li Y, Xiaomei L, Haiyan W: Possible mechanisms explaining the tendency towards interstitial fibrosis in aristolochic acid-induced acute tubular necrosis. Nephrol Dial Transplant 2007;22:445–456.

25 Hertig A, Anglicheau D, Verine J, Pallet N, Touzot M, Ancel P, Mesnard L, Brousse N, Baugey E, Glotz D, Legendre C, Rondeau E, Dubois Y: Early epithelial phenotypic changes predict graft fibrosis. J Am Soc Nephrol 2008;19:1584–1591.

26 Burton CJ, Combe C, Walls J, Haris KP: Secretion of chemokines and cytokines by human tubular epithelial cells in response to proteins. Nephrol Dial Transplant 1999;14:2628–2633.